Asian Journal of Chemistry; Vol. 23, No. 12 (2011), 5595-5597

ASIAN JOURNAL OF CHEMISTRY

www.asianjournalofchemistry.co.in

Synthesis and Structural Study on Co Substituted ZnO Nanoscale Crystals†

V.D. MOTE[1], V.R. HUSE[1], Y. PURUSHOTHAM[2] and B.N. DOLE[1,*]

[1]Materials Research Laboratory, Department of Physics, Dr. Babasaheb Ambedkar Marathwada University, Aurangabad-431 004, India
[2]Centre for Materials for Electronics Technology, IDA Phase-II, Cherlapally, Hyderabad-500 051, India

*Corresponding author: Fax + 91 0240 2403224; Tel: +91 0240 2403384; E-mail: drbndole.phy@gmail.com

AJC-10340

Cobalt substituted ZnO nanopowders with compositional formula $Zn_{1-x}Co_xO$ (x = 0.00, 0.05 and 0.10) were prepared by co-precipitation method at low temperature. The crystal structure, lattice parameters and average grain size of pure and Co substituted ZnO nanopowders were determined by X-ray diffraction technique. The XRD results indicate that the samples have hexagonal (wurtzite) crystal structure and there is no secondary phases observed. The lattice parameters 'a' and 'c' decrease with increasing Co content, it may be due the larger ionic radii of Zn^{2+} as compared to the Co^{2+}. The X-ray density reduces with increasing Co concentration, indicating the homogeneous substitution of Co^{2+} for Zn^{2+} in wurtzite ZnO structure. The average grain size was estimated from width of XRD using Scherrer's equation, it is observed that the grain size decreases with increasing Co content. The parameter 'u' (z coordinate of the oxygen atoms) of the wurtzite structure of $Zn_{1-x}Co_xO$ increases linearly with increasing Co concentration. The parameter 'u' increases as strain increases with Co concentration owing to the lattice distortion.

Key Words: Nanoscale crystals, X-ray density, u parameter, Strain.

INTRODUCTION

The quest of material for spintronics application that exploit both the magnetic moment and the charge of the electron, diluted magnetic semiconductors (DMSs) attracted much attention. The wide band gap of semiconductors, doping of transition metal (Mn, Co, Fe and V) have become one of the most extensively component for physicist.

The introduction of transition metal dopants into wide band gap oxides and III-V semiconductors have been shown to propagate carrier induced ferromagnetism[1,2]. Zinc oxide is attracting lot of attention of researchers, scientists and technologists owing to its potential applications such as gas sensors, photodetectors, light emitting diodes, varistors, piezoelectric devices and spin electronics[3-9]. In most of the cases, the transition metals doped ZnO samples are grown, employing complex and expensive techniques like molecular beam epitaxy metal-organic vapour phase epitaxy or pulsed laser deposition that require high grown temperatures, thermal hydrolysis technique[10], spray pyrolysis[11], chemical vapour deposition[12], thermal evaporation of Zn[13], hydrothermal synthesis[14,15], low temperature wet-chemical reaction[16]. However, most of these methods require a strictly controlled synthesis environment, expensive equipment and complicated procedures. We prefer co-precipitation method because it is a simple, low cost effective, easy handling and takes less time for the synthesis of the samples. We have undertaken a series of $Zn_{1-x}Co_xO$ with compositions (x = 0.00 0.05 and 0.10) for the investigations because less studies on Co doped ZnO nanoparticles are available in literature. It is not clear yet upto what % Co persists wurtzite structure in ZnO with this view we wish to throw more light on Co doped ZnO nanoscale crystals.

EXPERIMENTAL

The samples $Zn_{1-x}Co_xO$ (x = 0.00 0.05 and 0.10) nanocrystalline powders were prepared by co-precipitation method by the reaction of Zn^{2+} and OH^- in an alcoholic medium (methanol). Doping of magnetic elements was carried out by the addition of Co^{2+} to the reaction. Two ethanolic solutions, one containing $Zn(NO_3)_2 \cdot 6H_2O$ and $Co(NO_3)_2 \cdot 6H_2O$ and the other containing NaOH, were slowly mixed and heated for 2 h in a closed vessel for crystal growth. The Co concentrations were varied in the range 0.00-0.10. The precipitates were separated from the solution, washed with distilled water repeatedly to remove $NaNO_3$ as a secondary product and finally dried at 70 ºC in an oven to obtain ZnO nanometer-sized crystals. The nanocrystalline samples were annealed at 400 ºC

†Presented to the National Conference on Recent Advances in Condensed Matter Physics, Aligarh Muslim University, Aligarh, India (2011).

in air for 8 h. The crystal structure of the synthesized sample was studied using X-ray diffractometer (Model: PW-3710) employing CuK_α (λ = 1.5406 Å) radiation.

RESULTS AND DISCUSSION

The XRD patterns of $Zn_{1-x}Co_xO$ (x = 0.00 0.05 and 0.10) samples sintered at the 400 ºC temperature are shown in Fig. 1. All the patterns are found to have hexagonal wurtzite structure, without any additional impurity phases, thereby indicating that the wurtzite structure might have not affected due to the substitution of cobalt. Further, as no excess peaks were detected, one may say that all the starting organic precursors might have been completely decomposed. The lattice constants a and c show a slightly decreasing trend. It is observed that the lattice parameters decrease as Co content increases; the lattice parameters show a linear decrease, which is indication of the substitution of Co in the ZnO lattice site, according to Vegard's law. These results indicate that the substitutional property of the Co for Zn in ZnO samples. The decrement of lattice parameters a and c with increasing Co content is shown in Fig. 2.

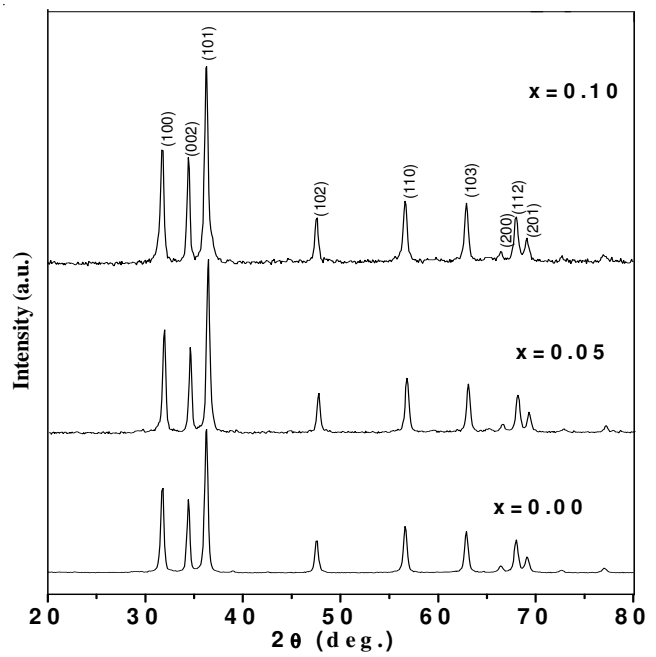

Fig. 1. X-ray diffraction patterns of $Zn_{1-x}Co_xO$ samples

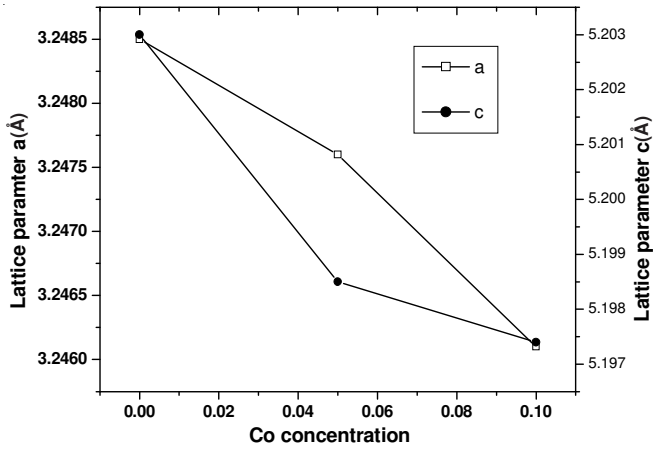

Fig. 2. Lattice parameters a and c *vs.* Co concentration of $Zn_{1-x}Co_xO$ samples

The lattice constants a and c decrease due to the larger ionic radius of Co are in good agreement with the Vegard's law. The unit cell volume is calculated from the lattice constants. However, for all samples the unit cell volume also goes on decreasing with increasing Co content is shown in Fig. 3. The decrement of the unit cell volume is correlated with the ionic radii: of Co. The X-ray density was estimated using the molecular weight and unit volume cell. The X-ray density goes on decreasing with increasing the Co concentration. It may be due to the decreasing the unit volume cell. The values of X-ray density and unit volume cell are tabulated in Table-1.

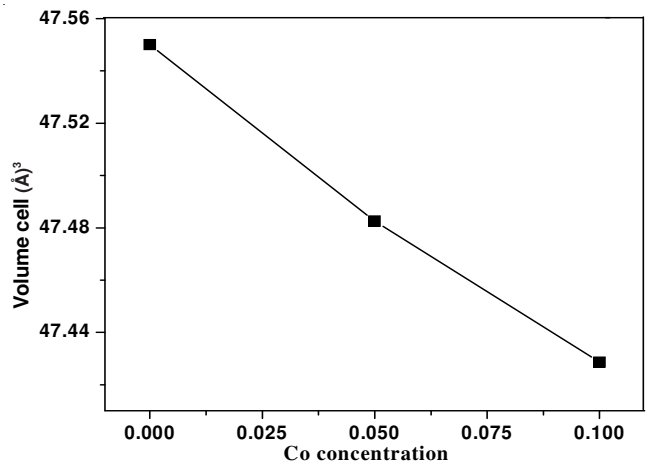

Fig. 3. Unit volume cell *vs.* Co concentration of $Zn_{1-x}Co_xO$ samples

TABLE-1
WURTZITE LATTICE PARAMETERS, AVERAGE GRAIN SIZE, VOLUME CELL, X-RAY DENSITY CALCULATED FROM XRD PATTERNS OF $Zn_{1-x}Co_xO$ SAMPLES

Samples	a (Å)	c (Å)	Grain size D (nm)	Volume (Å)^3	X-density (g/cm^3)
0.00	3.2485	5.2030	30.40	47.5500	5.6859
0.05	3.2476	5.1985	26.26	47.4825	5.6714
0.10	3.2461	5.1974	25.69	47.4286	5.6553

The average grain size of Co doped ZnO powders was determined from the extra broadening of the X-ray diffraction peaks of the sample using the Scherrer's formula applied to the strongest peak ($D = 0.9\ \lambda/\beta \cos\theta$, where D is crystallite size, λ is the wavelength of the X-rays, β is the full-width at half maximum intensity of the peak and θ is the diffraction angle). The average grain sizes of ZnCoO are found in the range 25-30 nm for 0.0-0.10 concentration respectively. It means that average grain size decreases with increasing Co content is summarized in Table-1.

The structural model was taken from the wurtzite ZnO in space group of $p6_3mc$ and both Zn/Co and O at 2b Wyckoff special position (1/3, 2/3, 0) and oxygen occupies the special position (1/3, 2/3, u)[17]. Therefore, u can be interpreted as the relative shift of the anionic sublattice to the cationic sublattices in z direction. In the literature values[18,19] for u of 0.3817- 0.3819 are found. Kisi and Elcombe presented a correlation $u(c/a) = \sqrt{3/8}$ for u with the lattice constant ratio c/a derived from geometrical considerations on the basis of a hexagonal close packing. They present values of own measurements and literature values of differently prepared ZnS and ZnO samples.

The decrease of c/a with larger u is much less pronounced for our samples compared to Kisi and Elcombe's results. Similar results have been published[17] for one sample of nanocrystalline ZnO indicating a dependence of the c/a-u correlation on the reactants used in the used wet chemical synthesis. The ratio c/a as a function of dopant concentration decreases generally with increasing dopant content is tabulated in Table-2. The c/a ratio from that of ideal value, the hexagonal lattice is further deformed upon Co substitution. From existing wurtzite structures, it is well known that when the bonding character becomes more ionic, c/a ratio moves further from the ideal value[18,19]. From the values of u further insight into the structure can be obtained. Only in an ideal wurtzite crystal structure with c/a = 1.6333 and u = 3/8 all Zn-O bond lengths are identical. For deviations in c/a and u the Zn-O bond in the c-axis direction is different in comparison with the other Zn-O bond lengths.

The distortion parameter has been calculated from the XRD data using the relation[20]

$$\varepsilon_v = \frac{(a^2c - a_0^2c_0)}{a_0^2c_0}$$

where, a_0 = 3.249Å and c_0 = 5.205Å for bulk samples. Due to difference in the ionic radii of the host (Zn^{2+}) and dopant (Co^{2+}) ions, there could be some distortion in the local lattice. The change in the distortion parameter of $Zn_{1-x}Co_xO$ nanoscale crystal particles with the change in the dopant ion concentration has been presented in Table-2, showing a decrease in lattice distortion parameter.

TABLE-2
c/a RATIO, u PARAMETER, LATTICE DISTORTION AND STRAIN CALCULATED FROM XRD DATA OF $Zn_{1-x}Co_xO$ SAMPLES

Samples	c/a ratio	u parameter	Lattice distortion	Strain
0.00	1.60217	0.382216	-0.00069	0.001276
0.05	1.60166	0.382336	-0.00212	0.001255
0.10	1.60072	0.382560	-0.00321	0.001336

XRD can be utilized to evaluate peak broadening with lattice strain due to dislocation[21]. The breadth of the Bragg peak is a combination of both instrument and sample dependent effects. Strain induced broadening is arising from crystal imperfection and distortion was calculated using the Stokes and Wilson formula[22] given as:

$$\varepsilon = \frac{\beta_{hkl}}{4\tan\theta}$$

It indicates that the lattice strain or microstrains of the prepared samples goes on increasing with increasing Co content. It may be due to the decreasing the grain size *i.e.* increasing the surface area. The lattice strains for all samples are given in the Table-2. The most significant contribution to the lattice strain in nanocrystalline $Zn_{1-x}Co_xO$ samples of the present study is from dislocations.

Conclusion

The nanocrystalline $Zn_{1-x}Co_xO$ samples were prepared successfully by co-precipitation method sintered at 400 ºC. The XRD result reveals that the prepared samples have wurtzite (hexagonal) structure and no any extra impurities phases. The wurtzite lattice parameters go on decreasing with increasing Co content. It indicates that the substitution of Co in ZnO samples. The X-ray densities are slightly decreasing with increasing Co in ZnO nanoscale crystals. It may be due to the smaller ionic radii of Co^{2+} ions as compared to the Zn^{2+} ions. The average crystallite sizes are found in the range 25-30 nm for Co concentration. The u parameter goes on increasing with increasing cobalt doping, it is due to the decreasing c/a ratio. The strain of nanocrystalline $Zn_{1-x}Co_xO$ crystals are increasing with enhancing the Co doping. It is found that the decrease in the crystalline size and enhancement in the lattice strain of the samples due to decreasing in lattice distortion.

REFERENCES

1. Y. Oho, D.K. Young, B. Beshoten, F. Matsukura, H. Ohno and D.I. Awschalom, *Nature*, **402**, 790 (1999).
2. S.J. Pearton, C.R. Abernathy, M.E. Overberg, G.T. Thaler, D.P. Norton, N. Theodoropoulou, A.F. Hebard, Y.D. Park, F. Ren, J. Kim and L.A. Boatner, *J. Appl. Phys.*, **93**, 1 (2003).
3. H.W. Lehman and R. Widmer, *J. Appl. Phys.*, **44**, 3868 (1973).
4. S. Liang, H. Sheng, Y. Liu, Z. Hio, Y. Lu and H. Shen, *J. Cryst. Growth*, **225**, 110 (2001).
5. N. Saito, H. Haneda, T. Sekiguchi, N. Ohashi, I. Sakagushi and K. Koumoto, *Adv. Mater.*, **14**, 418 (2002).
6. E. Olsson and G. Dunlop, *J. Am. Ceram. Soc.*, **76**, 65 (1993).
7. Z.L. Wang and J.H. Song, *Science*, **312**, 242 (2006).
8. K.M. Krishnan, A.B. Pakhomov, Y. Bao, P. Blomqvist, Y. Chun, M. Gonzales, K. Griffin, X. Ji and B.K. Roberts, *J. Mater. Sci.*, **41**, 793 (2006).
9. V.R. Palkar, *Nanostruct. Mater.*, **11**, 369 (1999).
10. H.K. Park, D.K. Kim and C.H. Kim, *J. Am. Ceram. Soc.*, **80**, 743 (1997).
11. T.T. Kodas, *Adv. Mater.*, **6**, 180 (1989).
12. B.P. Zhang, N.Y. Binh, K. Wakatsuki, Y. Segawa, Y. Yamada, N. Usami, M. Kawasaki and H. Koinuma, *J. Phys. Chem. B*, **108**, 10899 (2004).
13. G.Z. Shen, Y. Bando and Ch. J. Lee, *J. Phys. Chem. B*, **109**, 10578 (2005).
14. S.I. Hirano, *Ceram. Bull.*, **66**, 1342 (1987).
15. H. Zhang, D.R. Yang, D.S. Li, X.Y. Ma, S.Z. Li and D.L. Que, *Cryst. Growth Des.*, **2**, 547 (2005).
16. B. Liu and H.C. Zeng, *Langmuir*, **20**, 4196 (2004).
17. J.U. Brehm, M. Winterer and H. Hahn, *J. Appl. Phys.*, **100**, 064311 (2006).
18. E.M. Bachari, G. Baud, S B. Amor and M. Jacquet, *Thin Solid Films*, **348**, 165 (1999).
19. C. Kiener, M. Kurtz, H. Wilmer, C. Hoffmann, H.W. Schmidt, J.-D. Grunwaldt, M. Muhler and F. Schüth, *J. Catal.*, **216**, 110 (2003).
20. M. Diaconu, H. Schmidt, A. Poppl, R. Bottcher, J. Hoentsch, A. Rahm, H. Hochmuth, M. Lorenz and M. Grundmann, *Super Latt. Microstr.*, **38**, 413 (2005).
21. T. Ungar, A. Borbely, G.R.G. Muginstein, S. Berger and A.R. Rosen, *Nanostruct. Mater.*, **11**, 103 (1999).
22. A.R. Stokes and A.J.C. Wilson, *Proc. Phys. Soc.*, **56**, 174 (1944).